between 0.77 and 0.93 (*21*). Because LECS and MECS energy ranges partially overlap, the LECS constant was free to vary. The goodness of the fit was quantized by the χ^2 test. The significance level of a model was obtained from the *F* test. An *F* probability greater than 99% implied a significant improvement of the fit.
24. P. Magdziarz, A. Zdziarski, *Mon. Not. R. Astron. Soc.* **273**, 837 (1995).
25. M. H. Ulrich, T. J.-L Courvoisier, W. Wamsteker, *Astron. Astrophys.* **204**, 21 (1988).
26. G. C. Perola *et al.*, *Astron. Astrophys.* **389**, 802P (2002).
27. N. I. Shakura, R. A. Sunyaev, *Astron. Astrophys.* **24**, 337 (1997).
28. F. Haardt, L. Maraschi, *Astrophys. J.* **380**, L51 (1991).
29. F. Haardt, L. Maraschi, *Astrophys. J.* **413**, 507 (1993).
30. J. Poutanen, R. Svensson, *Astrophys. J.* **470**, 249 (1996).
31. M. Dovciak *et al.*, *Mon. Not. R. Astron. Soc.* **350**, 745 (2004).
32. Haardt *et al.* (*16*) also reported a first indication of a steepening of the spectrum above 20 keV.
33. K. A. Arnaud, *Asp. Conf. Ser.* **101**, 17 (1996).
34. J. M. Dickey, F. J. Lockman, *Annu. Rev. Astron. Astrophys.* **28**, 215 (1990).
35. P. Grandi, M. Guainazzi, *3C 273 BeppoSAX-ASCA intercalibration* (1990), available at www.asdc.asi.it/bepposax/software/cookbook.
36. The authors thank M. Fiocchi for helping with the data reduction and M. Cappi, M. Dadina, L. Foschini, and G. Malaguti for discussions and constructive criticism. Thanks are also due to L. Amati for helping with a problem in statistics. Financial support from the Italian Space Agency (ASI/n.045) and Ministero Università Ricerca Scientifica Tecnologica is gratefully acknowledged. G.G.C.P. gratefully acknowledges CNRS and the Centre d'Etude Spatial de Rayonnement in Toulouse for hospitality and partial financial support.

Supporting Online Material
www.sciencemag.org/cgi/content/full/306/5698/998/DC1
Figs. S1 to S5

22 June 2004; accepted 7 October 2004

Energy Transfer Across a Metal Film Mediated by Surface Plasmon Polaritons

P. Andrew* and W. L. Barnes†

Coupled surface plasmon polaritons (SPPs) are shown to provide effective transfer of excitation energy from donor molecules to acceptor molecules on opposite sides of metal films up to 120 nanometers thick. This variant of radiative transfer should allow directional control over the flow of excitation energy with the use of suitably designed metallic nanostructures, with SPPs mediating transfer over length scales of 10^{-7} to 10^{-4} meters. In the emerging field of nanophotonics, such a prospect could allow subwavelength-scale manipulation of light and provide an interface to the outside world.

Thin metal films and nanostructures exhibit remarkable optical properties due to the plasmon modes they support. Recent observations of single-molecule surface-enhanced Raman scattering (*1*, *2*) rely on the enhanced optical fields associated with these modes. The extraordinary transmission of light through subwavelength-hole arrays (*3*, *4*) and the enhanced transmission of fluorescence through continuous metal films (*5*–*7*) also involve SPPs. We show that these modes can mediate excitation energy transfer between molecules on opposite sides of a metallic film, allowing controlled radiative transfer over distances much greater than the usual nonradiative Förster energy transfer range of ≤10 nm. With recent developments in SPP waveguides (*8*–*12*), this offers exciting possibilities for controlling the optical interaction between molecules in areas as diverse as photosynthesis (*13*) and solid-state polymer lasers (*14*).

Excitation energy transfer from donor to acceptor molecules separated by a distance *r* may proceed in three ways. Dexter transfer (*15*), based on wave-function overlap, has an exponential distance dependence with a range of ~1 nm. Förster transfer (*16*, *17*), a near-field resonant dipole-dipole interaction, has greater range, on the order of 10 nm, falling as $1/r^6$. Dexter and Förster transfer are nonradiative, in contrast with the final process, radiative transfer, which is the simple emission and absorption of a photon and has the longest range, falling as $1/r^2$. It has been shown that the local optical environment (*18*, *19*) modifies the Förster process; the transfer rate is measured to be proportional to the optical density of states (*20*). Despite this, the Förster process lacks the range to allow energy transfer over distances of >10 nm; only radiative transfer has sufficient range. Unfortunately, the probability of such transfer is usually low and the directionality cannot be controlled. For controllable directional transfer, a waveguide is needed to direct the photon (polariton) from the donor to the acceptor.

SPPs are guided electromagnetic waves that propagate along interfaces between metals and dielectrics and have propagation lengths up to 10^{-4} m. The near-fields of the donor dipole moment couple to the SPP mode efficiently; for planar metallic surfaces, SPP excitation can account for >95% of the total dipole emission (*21*). We show that coupled SPPs are efficient mediators of molecular excitation energy transfer between donor and acceptor molecules on opposite sides of metallic films up to 120 nm thick (usual transmittance <1%).

Our structures (Fig. 1A) consist of donor- and acceptor-doped dielectric layers separated by silver films thick enough to prohibit Förster transfer. The donor dye Alq_3 was dispersed in polymethylmethacrylate (PMMA) (4% weight; 6.35×10^{19} molecules/cm^3) and spun cast onto silica substrates to form 60-nm-thick films. Silver films 30 to 120 nm in thickness were thermally evaporated on the donor layer and capped with spun-cast 60-nm-thick layers containing the acceptor dye rhodamine 6G (R6G) doped into PMMA (1.6% weight; 2.54×10^{19} molecules/cm^3). Identical donor-only and acceptor-only control samples were also fabricated.

Similar refractive index dielectrics were used on either side of the silver film (n_{PMMA} = 1.49, n_{SiO_2} = 1.46 for light of wavelength λ = 632.8 nm) to ensure that the SPPs associated with each metal interface interact to produce two coupled SPP modes, one with symmetric and the other with antisymmetric magnetic fields (*22*). The fields of these coupled SPPs [Fig. 1A, calculated (*23*) for the peak donor emission wavelength] span the metal film, extending through both the donor and acceptor layers, and thus mediate the energy transfer in our samples.

Calculation of the power dissipation spectrum of a dipole source within the donor layer (*24*) of our samples shows that the dominant decay channel is the excitation of coupled SPP modes. Peaks in this spectrum (Fig. 1B) represent coupling of the source to SPP modes, the area under each peak indicating that 6 and 70% of the total dipole energy are coupled to the symmetric and antisymmetric SPPs, respectively. Evaluation of the modal dispersion (*25*) shows two coupled SPPs beyond the light line (Fig. 1C).

Figure 1D shows the photoluminescence (PL) spectra of donor (Alq_3) and acceptor (R6G) doped PMMA films and the acceptor absorption spectrum. PL spectra were recorded with a fiber-coupled spectrometer/charge-coupled device system with spectral resolution of 1 nm, with a continuous wave

Thin Film Photonics, School of Physics, University of Exeter, Stocker Road, Exeter, EX4 4QL, UK.

*Present address: The Nanoscience Centre, University of Cambridge, JJ Thompson Avenue, Cambridge, CB3 0FF, UK.
†To whom correspondence should be addressed. E-mail: w.l.barnes@exeter.ac.uk

diode laser pump source. The pump wavelength (408 nm) corresponds to a R6G absorption minimum, minimizing direct excitation of the R6G. Samples were pumped from the substrate side and PL collected from the opposite side.

The simplest evidence of energy transfer is the observation of the emission spectrum of the acceptor after donor excitation. Figure 2 shows the PL spectra recorded for donor/acceptor and control samples. The Alq_3 control spectrum accounts for the donor signal overlapping the acceptor spectrum, the R6G control for the directly excited acceptor emission. Comparing these spectra, we obtain the energy transfer acceptor signal. Data are shown for several silver film thicknesses to illustrate the effect of changing the degree of coupling of the SPPs.

The control spectra show the usual Alq_3 and R6G PL. The Alq_3 spectra (peak 520 nm) dominate the R6G spectra (peak 565 nm) for all silver thicknesses as expected given that the pump laser matches the Alq_3 absorption band but not the R6G. Furthermore, the pump beam is attenuated strongly by the silver film for the R6G-only sample. In contrast, the spectra from the samples containing both donors and acceptors display the characteristic emission of both Alq_3 and R6G; the R6G emission is substantially increased compared with that of the control; in the case of the 60-nm silver film, this acceptor emission is increased by an order of magnitude. This enhanced acceptor emission demonstrates that energy is being efficiently transferred from the Alq_3 to the R6G through the silver film. Figure 2 shows that the energy transfer has a strong dependence on silver film thickness. If the areas under the donor/acceptor, donor-only, and acceptor-only spectra from 440 to 750 nm are I_{DA}, I_D, and I_A, respectively, then the energy transferred is $I_{DA} - fI_D - I_A$, with efficiency $(I_{DA} - fI_D - I_A)/I_D$ compared with direct donor emission through the film. Finally, $(I_{DA} - fI_D - I_A)/I_{DA}$ gives the proportion of the total donor/acceptor sample emission attributable to energy transfer. These values are given as a function of silver thickness in Table 1. The correction factor f accounts for the decrease in Alq_3 emission intensity in the donor/acceptor sample spectra compared with the Alq_3 control spectrum, given that it is the ratio of the donor emission intensities at 520 nm in the two spectra.

Table 1 shows that although the absolute amount of energy transferred decreases as the silver thickness increases, the transfer signal is most significant for intermediate silver thicknesses, peaking for 60-nm-thick films in which transfer accounts for 70% of the total emission. This behavior results from an interplay between the probability of direct emission through the film (falling exponentially with silver thickness) and that of transfer by means of SPP modes. This process has a complex distance dependence, and modeling reveals that this arises because of variation of the dipolar coupling strength to the SPPs with increasing silver thickness. For thin silver films (<30 nm), the symmetric coupled SPP is strong but extremely sharp, whereas the antisymmetric SPP is broad but weak. As the silver thickness increases, the symmetric mode weakens and broadens, whereas the antisymmetric mode sharpens and intensifies, leading to increasing dipolar coupling for silver films up to 60 nm thick, at which point coupling to the symmetric mode starts to decrease. This nonmonotonic variation in dipolar coupling to the SPP modes is responsible for the observed dominance of SPP-mediated energy transfer over direct emission for intermediate silver thicknesses.

The energy-transfer process was also monitored by measuring the temporal evolution of the spectrally resolved donor and acceptor emission. For our chosen system, Alq_3 has a significantly longer lifetime (τ = 15.4 ns) than that of R6G (τ = 0.6 ns); thus, directly excited acceptor R6G emission should die away within a few nanoseconds. Subsequent acceptor emission must therefore arise from energy transfer from the longer lived excited donor population.

Time-resolved emission data were recorded with time-correlated single-photon counting after pulsed excitation by a 440-

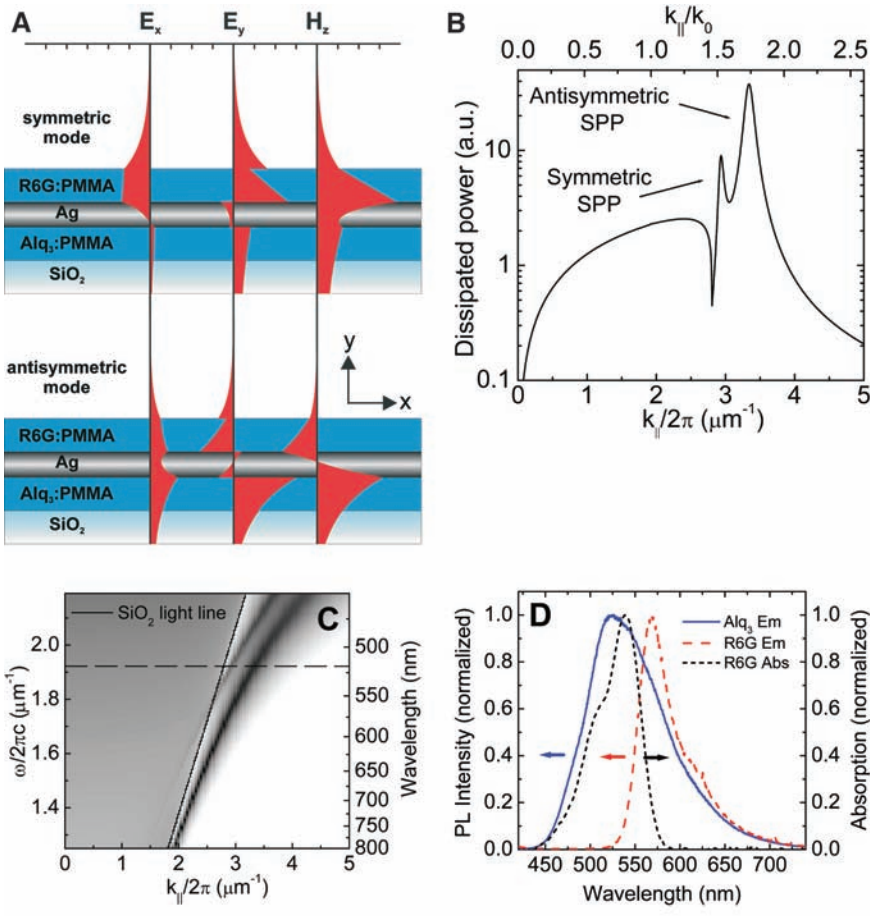

Fig. 1. Coupled SPP modes supported by a dielectric-clad thin silver film. (**A**) Schematic sample cross sections superposed with field profiles associated with the symmetric (top) and antisymmetric (bottom) coupled SPPs (calculated for maximum Alq_3 emission, λ = 520 nm) illustrating how the fields span the silver film. For clarity, the antisymmetric SPP fields are expanded by a factor of 2. In all calculations, a 60-nm-thick silver film (with complex optical permittivity $\varepsilon = -9.39 + 0.78i$) is bounded by 80-nm-thick PMMA layers ($\varepsilon = 2.22 + 0i$), supported by a semi-infinite silica substrate ($\varepsilon = 2.12 + 0i$). (**B**) Power dissipation spectrum calculated for an isotropic dipole source (λ = 520 nm) embedded centrally within the donor layer. Dipolar power dissipation [arbitrary units (a.u.)] is plotted against the in-plane wave vector component of the dipole field ($k_{||}/2\pi$, absolute value; $k_{||}/k_0$, scaled to the free-space photon wave vector). Peaks correspond to excitation of the symmetric and antisymmetric SPP modes. (**C**) Gray-scale plot of power dissipation spectra as a function of donor emission frequency ($\omega/2\pi c$) showing dispersion of the coupled SPP modes. Black corresponds to high power loss; the dotted line shows the wavelength corresponding to the calculation shown in (B). (**D**) Absorption and emission spectra (black and red) of a 60-nm-thick R6G-doped PMMA film (acceptor) together with the emission spectrum (blue) of an Alq_3-doped PMMA film (donor). Arrows indicate the relevant axis for each spectrum.

nm diode laser, with the use of interference filters to spectrally isolate donor and acceptor emission. Figure 3 shows the temporal evolution of the emission intensity in the spectral region associated with acceptor emission for the donor/acceptor and donor-only/acceptor-only control samples (60-nm-thick silver film). The donor-only decay is the weakest because the donor emits very little at this wavelength (Fig. 1D) and is also strongly attenuated by the filter used. The temporal behavior of these decay curves is complex because they result from the decay of distributions of excited dye molecules with differing local photonic environments. A biexponential function was therefore fit to the experimental data, with the majority component being the lifetime quoted. The acceptor-only decay is relatively short, whereas that in the presence of donors shows a strong long-lifetime component with similar lifetime to that of the major component of the donor-only decay curve (τ = 13.9 ns). This implies that the long-lived acceptor emission arises from energy transfer between long-lived excited donors on one side of the silver film and acceptors on the other. Together with the emission spectra (Fig. 2), these data provide strong evidence for energy transfer between donors and acceptors across the silver film. Though diminished, transfer is still present in samples with a silver film thickness of 120 nm. Subsequent time-resolved measurements of the Alq_3 emission from the donor-only and donor/acceptor samples show similar lifetimes in both environments (τ = 14.7 ns and τ = 15.5 ns, respectively). This suggests that the energy-transfer process does not directly quench the donor molecules, indicating the transfer to be radiative rather than Förster.

The data shown in Figs. 2 and 3 demonstrate energy transfer but do not identify the modes responsible. To address this, we fabricated a range of identical structures with corrugated rather than planar silica substrates; the corrugation (period 368 nm, depth 60 nm) allows the bound SPP modes to couple to free photons by means of scattering. Deposition of the initial spun-cast PMMA layer partially planarized this corrugation—the silver film corrugation depth was ~10 nm—as measured by atomic force microscopy. The optical modes were explored by measuring the transmittance as a function of frequency and in-plane wave vector (*26*) to build up a dispersion diagram. Such measurement on a donor/acceptor sample with a silver film thickness of 60 nm (Fig. 4A) shows the presence of the coupled SPP modes (Fig. 1B) as rapidly dispersing bands of increased transmission (100 times the off-resonance value), which have been scattered by the grating.

Measurement of angle-resolved PL spectra as a function of emission angle (0.5° resolution) to build PL-based dispersion diagrams reveals the extent to which the coupled SPPs are involved in the emission from and transfer between the dye layers. An example of such data for the donor/acceptor sample with a silver film thickness of 60 nm is shown in Fig. 4B. The resemblance of these data to those of Fig. 4A is strong with the emission dominated by reradiation from grating-scattered coupled SPP modes. Below λ = 550 nm, the sole emission is the strong reradiation of coupled SPP modes excited by

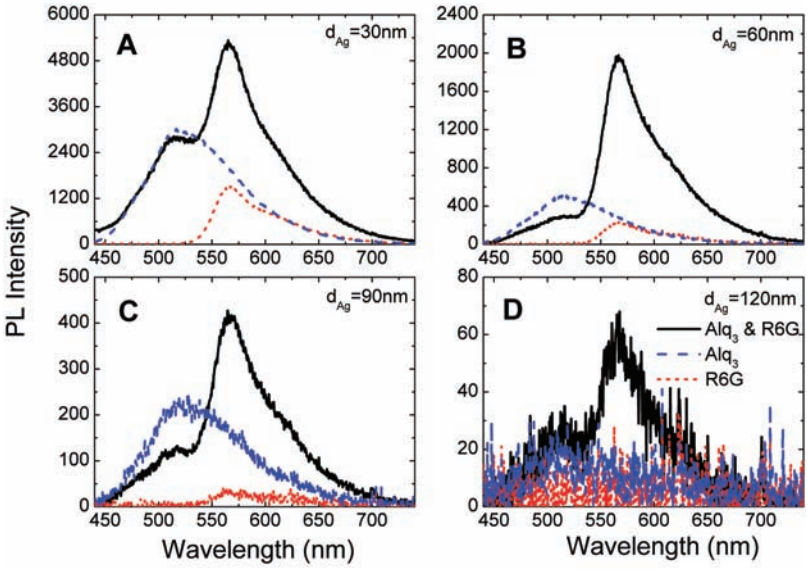

Fig. 2. (**A** to **D**) PL spectra from planar samples with silver films of thickness 30, 60, 90, and 120 nm (arbitrary intensity units). In each case, data are shown for donor-only samples (Alq_3:PMMA|Ag|PMMA) (blue spectra), acceptor-only samples (PMMA|Ag|R6G:PMMA) (red spectra), and samples containing both donor and acceptor layers (Alq_3:PMMA|Ag|R6G:PMMA) (black spectra).

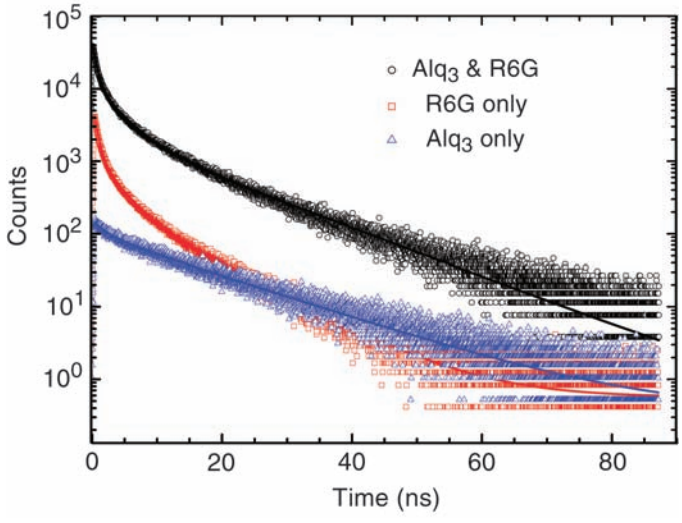

Fig. 3. Time-resolved PL of samples with a silver film thickness of 60 nm measured in the spectral region dominated by acceptor emission (λ > 648 nm). Data are shown for donor-only, acceptor-only, and donor and acceptor samples.

Table 1. Efficiency of energy transfer through silver films as a function of the silver thickness.

Silver thickness (nm)	Energy transfer		
	Absolute value of $I_{DA} - fI_D - I_A$ (normalized to 120-nm value)	Fraction of direct donor emission $(I_{DA} - fI_D - I_A)/I_D$	Fraction of total emission $(I_{DA} - fI_D - I_A)/I_{DA}$
30	124	0.47	0.27
60	90	2.11	0.70
90	16	0.74	0.52
120	1	0.42	0.22

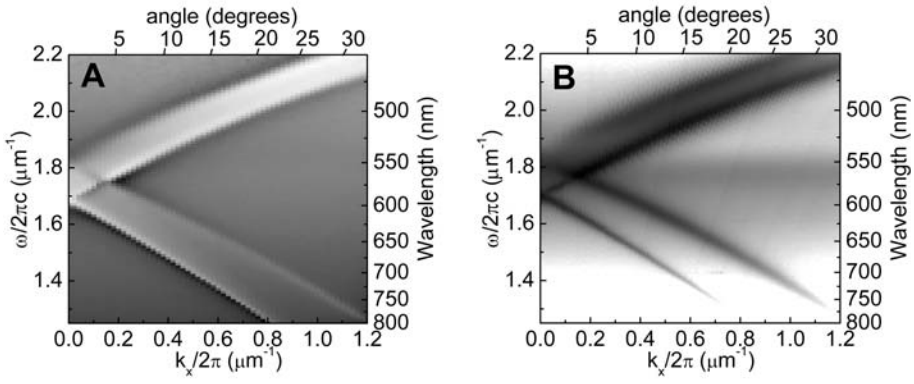

Fig. 4. Dispersion data for the sample containing both donors and acceptors with structure Alq_3:PMMA|60 nm Ag|R6G:PMMA deposited onto a corrugated substrate. Data were obtained by recording the transverse-magnetic polarized (**A**) transmittance and (**B**) PL emission as a function of the in-plane wave vector of light, $k_x/2\pi$. Both are plotted with a logarithmic gray scale, where for (A), transmittance ranges from $T = 0.001$ (black) to $T = 0.1$ (white), whereas for (B), white represents minimum and black maximum PL emission. In each case, the data are dominated by the scattered features corresponding to the excitation and emission of both symmetric and antisymmetric coupled SPPs.

donor molecules on the far side of the silver film, whereas above $\lambda = 550$ nm there are two components to consider. In addition to the strong coupled SPP reradiation, which now arises from SPPs generated by the relaxation of acceptor molecules on the near side of the silver film (primarily excited by energy transferred from the donors), there is a broad emission band from $\lambda = 550$ to 675 nm, peaking at ~565 nm, which does not disperse with angle. This band is an order of magnitude more intense than for the acceptor-only sample (*27*) and corresponds to the enhanced acceptor emission previously seen in Fig. 2. This emission is direct radiation from acceptor molecules rather than grating-scattered reradiation from acceptor-excited SPP modes. Figure 4B clearly shows that both donors and acceptors strongly excite the coupled SPP modes of the structure, that strong acceptor emission arises from excitation of the remote donor layer, and that the total emission from the structure can be strongly enhanced by recovering coupled SPP emission from both donor and acceptor through scattering from the grating microstructure.

A direct application of the strategy outlined above would be to top-emitting organic light-emitting diodes. Such devices are attractive for display applications where emission occurs through a metallic cathode. We have shown that depositing a dielectric layer on the surface of the device may lead to greater efficiency (*7*), and by dye-doping this layer SPP-mediated energy transfer could increase the spectral coverage of the output. Another potential area of application is synthetic light harvesting structures; SPP modes could act to channel energy from absorbing species to reaction centers and more generally in photochemistry near surfaces.

References and Notes

1. H. X. Xu, E. J. Bjerneld, M. Kall, L. Borjesson, *Phys. Rev. Lett.* **83**, 4357 (1999).
2. S. M. Nie, S. R. Emery, *Science* **275**, 1102 (1997).
3. T. W. Ebbesen, H. J. Lezec, H. F. Ghaemi, T. Thio, P. A. Wolff, *Nature* **391**, 667 (1998).
4. W. L. Barnes, W. A. Murray, J. Dintinger, E. Devaux, T. W. Ebbesen, *Phys. Rev. Lett.* **92**, 107401 (2004).
5. R. W. Gruhlke, W. R. Holland, D. G. Hall, *Phys. Rev. Lett.* **56**, 2838 (1986).
6. D. K. Gifford, D. G. Hall, *Appl. Phys. Lett.* **81**, 4315 (2002).
7. S. Wedge, J. A. E. Wasey, I. Sage, W. L. Barnes, *Appl. Phys. Lett.* **85**, 182 (2004).
8. R. Charbonneau, P. Berini, E. Berolo, E. Lisicka-Shrzek, *Opt. Lett.* **25**, 844 (2000).
9. J. C. Weeber *et al.*, *Phys. Rev. B* **64**, 045411 (2001).
10. H. Ditlbacher, J. R. Krenn, G. Schider, A. Leitner, F. R. Aussenegg, *Appl. Phys. Lett.* **81**, 1762 (2002).
11. S. I. Bozhevolnyi, V. S. Volkov, *Opt. Lett.* **26**, 734 (2001).
12. W. L. Barnes, A. Dereux, T. W. Ebbesen, *Nature* **424**, 824 (2003).
13. J. R. Oppenheimer, *Phys. Rev.* **60**, 158 (1941).
14. M. Meier *et al.*, *Appl. Phys. Lett.* **74**, 7 (1999).
15. D. Dexter, *J. Chem. Phys.* **21**, 836 (1953).
16. T. Förster, *Annalen der Physik* **2**, 55 (1948).
17. T. Förster, *Discuss. Faraday Soc.* **27**, 7 (1959).
18. C. E. Finlayson, D. S. Ginger, N. C. Greenham, *Chem. Phys. Lett.* **338**, 83 (2001).
19. M. Hopmeier, W. Guss, M. Deussen, E. O. Göbel, R. F. Mahrt, *Phys. Rev. Lett.* **82**, 4118 (1999).
20. P. Andrew, W. L. Barnes, *Science* **290**, 785 (2000).
21. W. H. Weber, C. F. Eagen, *Opt. Lett.* **4**, 236 (1979).
22. D. Sarid, *Phys. Rev. Lett.* **47**, 1927 (1981).
23. J. B. Harris, T. W. Preist, J. R. Sambles, *J. Opt. Soc. Am. A* **12**, 1965 (1995).
24. G. W. Ford, W. H. Weber, *Phys. Rep.* **113**, 195 (1984).
25. W. L. Barnes, *J. Mod. Opt.* **45**, 661 (1998).
26. M. G. Salt, W. L. Barnes, *Opt. Commun.* **166**, 151 (1999).
27. P. Andrew, W. L. Barnes, data not shown.

28. We thank M. J. Jory for the R6G absorption spectrum data presented in Fig. 1D and the UK EPSRC and the EC (under project FP6 NMP4-CT-2003-505699) for financial support.

20 July 2004; accepted 27 September 2004

Enhancement of Ferroelectricity in Strained $BaTiO_3$ Thin Films

K. J. Choi,[1] M. Biegalski,[2] Y. L. Li,[2] A. Sharan,[2] J. Schubert,[3] R. Uecker,[4] P. Reiche,[4] Y. B. Chen,[5] X. Q. Pan,[5] V. Gopalan,[2] L.-Q. Chen,[2] D. G. Schlom,[2] C. B. Eom[1]*

Biaxial compressive strain has been used to markedly enhance the ferroelectric properties of $BaTiO_3$ thin films. This strain, imposed by coherent epitaxy, can result in a ferroelectric transition temperature nearly 500°C higher and a remanent polarization at least 250% higher than bulk $BaTiO_3$ single crystals. This work demonstrates a route to a lead-free ferroelectric for nonvolatile memories and electro-optic devices.

Enormous strains can exist in thin films when one material is deposited on another (*1*), resulting from differences in crystal lattice parameters and thermal expansion behavior between the film and the underlying substrate or arising from defects formed during film deposition (*2*, *3*). As a result, the properties of thin films can be markedly different than the intrinsic properties of the corresponding unstrained bulk materials (*4*–*9*). Although such strain often leads to degraded film properties, if judicious use is made of substrates and growth parameters, strain offers the opportunity to enhance particular properties of a chosen material in thin film form, namely strain engineering.

Strain engineering could facilitate the introduction of more environmentally benign ferroelectric random-access memories (FeRAM). Large shifts in the paraelectric-to-

[1]Department of Materials Science and Engineering, University of Wisconsin–Madison, Madison, WI 53706, USA. [2]Department of Materials Science and Engineering, Pennsylvania State University, University Park, PA 16802, USA. [3]Institut für Schichten und Grenzflächen ISG1-IT, Forschungszentrum Jülich GmbH, D-52425 Jülich, Germany. [4]Institute for Crystal Growth, Max-Born-Straße 2, D-12489 Berlin, Germany. [5]Department of Materials Science and Engineering, The University of Michigan, Ann Arbor, MI 48109, USA.

*To whom correspondence should be addressed. E-mail: eom@engr.wisc.edu